



Brassinosteroid signaling integrates multiple pathways to release apical dominance in tomato

Xiaojuan Xia^{a,1}, Han Dong^{b,1}, Yanling Yin^{a,1}, Xuewei Song^{a,1}, Xiaohua Gu^a, Kangqi Sang^a, Jie Zhou^a, Kai Shi^a, Yanhong Zhou^a, Christine H. Foyer^{c,2}, and Jingquan Yu^{a,d,2}

^aDepartment of Horticulture, Zijingang Campus, Zhejiang University, Hangzhou 310058, P.R. China; ^bCollege of Horticulture, Northwest A&F University, Yangling, Shaanxi 712100, P.R. China; ^cSchool of Biosciences, College of Life and Environmental Sciences, University of Birmingham, B15 2TT Edgbaston, United Kingdom; and ^dKey Laboratory of Horticultural Plants Growth, Development and Quality Improvement, Agricultural Ministry of China, Zhejiang University, Hangzhou 310058, P.R. China

Edited by Jiayang Li, Institute of Genetics and Developmental Biology (Chinese Academy of Science), Beijing, China, and approved February 5, 2021 (received for review March 8, 2020)

The control of apical dominance involves auxin, strigolactones (SLs), cytokinins (CKs), and sugars, but the mechanistic controls of this regulatory network are not fully understood. Here, we show that brassinosteroid (BR) promotes bud outgrowth in tomato through the direct transcriptional regulation of *BRANCHED1 (BRC1)* by the BR signaling component *BRASSINAZOLE-RESISTANT1 (BZR1)*. Attenuated responses to the removal of the apical bud, the inhibition of auxin, SLs or gibberellin synthesis, or treatment with CK and sucrose, were observed in bud outgrowth and the levels of *BRC1* transcripts in the BR-deficient or *bzr1* mutants. Furthermore, the accumulation of BR and the dephosphorylated form of *BZR1* were increased by apical bud removal, inhibition of auxin, and SLs synthesis or treatment with CK and sucrose. These responses were decreased in the *DELLA*-deficient mutant. In addition, CK accumulation was inhibited by auxin and SLs, and decreased in the *DELLA*-deficient mutant, but it was increased in response to sucrose treatment. CK promoted BR synthesis in axillary buds through the action of the type-B response regulator, *RR10*. Our results demonstrate that BR signaling integrates multiple pathways that control shoot branching. Local BR signaling in axillary buds is therefore a potential target for shaping plant architecture.

axillary bud | *BRANCHED1* | cytokinin | *DWARF* | shoot architecture

Shoot architecture has significant impacts on light capture, photosynthesis, and resource allocation. Moreover, it is important in ensuring reproductive success and crop productivity (1–3). Optimizing shoot architecture is thought to be a promising approach for increasing crop yield to meet the challenges of an increasing global population and climate change (2). Shoot branching is mainly determined by the formation of axillary buds in the leaf axils, together with subsequent outgrowth or dormancy. The production of axillary buds is controlled genetically (4), while the outgrowth of axillary buds is controlled by a range of factors and displays a high level of plasticity in response to sugar availability, hormonal signals, and changing environment conditions (5, 6). Multiple pathways converge on a common transcription factor named *BRANCHED1 (BRC1)* to control bud outgrowth in different plant species (7). *BRC1* is expressed specifically in axillary buds and acts as a central regulator that inhibits bud outgrowth (8, 9).

The phytohormone regulatory network plays a principal role in regulating the outgrowth of axillary buds. The growth of buds is inhibited by auxin and strigolactones (SLs) and is promoted by cytokinins (CKs). To date, several hormone-based models have been used to explain the control of bud outgrowth. The canalization model proposes that auxin synthesized in the young leaves of shoot apex is transported basipetally through the main stem in a polar manner to inhibit shoot branching indirectly by competing for access to the main polar auxin transport stream (10, 11). The second messenger model proposes that CKs and SLs act downstream of auxin to control shoot branching. In this model,

local CK synthesis in the nodal stem is sufficient to promote axillary bud outgrowth, whereas auxin in the polar transport stream suppress CK synthesis by inhibiting the expression of *Isopentenyltransferase* (12). SLs are synthesized mainly in roots and transported acropetally to inhibit shoot branching (13–15). SLs synthesis is mediated by the sequential action of Carotenoid Cleavage Dioxygenase 7 (CCD7), Carotenoid Cleavage Dioxygenase 8 (CCD8) and the cytochrome P450 named More Axillary Growth1 (MAX1) (16). Notably, auxin signaling regulates the expression of SL synthesis genes (17, 18).

Recently, sugars were shown to be major players in the regulation of bud outgrowth. Sugar levels in the dormant buds increase when the buds start to grow before any changes in the auxin content are observed in the adjacent stem (19). However, internode elongation may inhibit shoot branching by diverting sugars away for the growing buds (20). Hence, genes regulating stem elongation, especially those related to gibberellin (GA) signaling, influence shoot branching (21, 22). Little information is available, however, concerning how hormone signaling and metabolic cues are linked to the regulation of *BRC1*.

Brassinosteroids (BRs) are a group of steroid hormones that play critical roles in plant growth and development (23). BR

Significance

For almost a century, auxin had been well-known as the master regulator of apical dominance. Recently, however, sugars were shown to be the initial regulator of apical dominance, while strigolactones (SLs) and cytokinins (CKs) act downstream of auxin to control bud outgrowth. However, the interactions of the different pathways have remained outstanding questions. Here, we report that brassinosteroids (BRs) are essential for the release of apical dominance in tomato. CK signaling relays information from auxin, SL, and sugars to promote the production of BRs, which activate the *BZR1* transcription factor to suppress the expression of *BRANCHED1*, an inhibitor of bud outgrowth. These findings demonstrate that hormonal and metabolic pathways impinge on a common BR signaling for controlling shoot branching.

Author contributions: X.X., Y.Z., and J.Y. designed research; H.D., Y.Y., X.S., X.G., and K. Sang performed research; J.Z. and K. Shi analyzed data; and X.X., C.H.F., and J.Y. wrote the paper.

The authors declare no competing interest.

This article is a PNAS Direct Submission.

This open access article is distributed under [Creative Commons Attribution-NonCommercial-NoDerivatives License 4.0 \(CC BY-NC-ND\)](https://creativecommons.org/licenses/by-nc-nd/4.0/).

¹X.X., H.D., Y.Y., and X.S. contributed equally to this work.

²To whom correspondence may be addressed. Email: C.H.Foyer@bham.ac.uk or jqyu@zju.edu.cn.

This article contains supporting information online at <https://www.pnas.org/lookup/suppl/doi:10.1073/pnas.2004384118/-DCSupplemental>.

Published March 8, 2021.

binding to the receptor Brassinosteroid Insensitive1 (BRI1) triggers a phosphorylation cascade that results in the inactivation of the negative regulator Brassinosteroid Insensitive2 (BIN2), leading to dephosphorylation and activation of the transcription factors BRASSINAZOLE RESISTANT1 (BZR1) and BRI1 EMS SUPPRESSOR1 (BES1) (24). Dephosphorylated BZR1 (dBZR1) can regulate the expression of a variety of genes involved in plant growth and development as well as stress responses (25–27). BR also promotes shoot branching. For example, the tissue-specific expression of the BR synthesis genes *CYP724B* and *CYP90B* increases tiller number in rice (28), whereas BR synthesis and signaling mutants have lower tiller numbers than the wild-type (WT) rice (29, 30). To date, relatively few studies have considered the mechanisms whereby BR regulates shoot branching. Recent studies have demonstrated that BES1 or BZR1 forms a complex with D53-like proteins, that are regulators of SL signaling, to inhibit the expression of *BRC1* in *Arabidopsis* or *FC1* in rice (31, 32). However, the precise role of BR synthesis and signaling in the control of shoot branching remains to be defined, and little is known about the interactions between BR and other hormone and sugar pathways in the shoot branching regulatory network.

Here, we show that the transcription factor BZR1 mediates BR to promote axillary bud outgrowth in tomato through the direct suppression of *BRC1*. Bud activation in response to a depletion of auxin/SLs levels or by treatment with CKs/sucrose is dependent on an increase in BR signaling. Conversely, enhanced GA signaling results in suppression of shoot branching, together with a decrease in BR and BZR1 levels. Auxin, SL, sucrose, and GA were found to regulate CK accumulation, which promoted the expression of BR biosynthesis gene through the type-B response regulator (RR), RR10. These findings demonstrate that multiple hormone and sugar signals interact to regulate shoot branching through a common BR–BZR1–*BRC1* signaling cascade.

Results

BR Biosynthesis and Signaling Promote Shoot Branching in Tomato.

We first determined whether BR regulates bud outgrowth in tomato. The *dwf* mutant that is defective in the BR biosynthesis gene *DWARF* (*DWF*) had significantly fewer lateral buds than the WT, while overexpression of *DWARF* (*OE-DWF*) promoted bud outgrowth (Fig. 1 *A* and *B*). Mutation of the BR signaling gene *BZR1* (*bzr1*) suppressed bud outgrowth, while overexpression of *BZR1* (*OE-BZR1*) significantly promoted bud outgrowth. Virus-induced gene silencing (VIGS) of homologs of *BIN2*, which is a negative regulator of BR signaling, revealed that *BIN2.2* is a suppressor of bud outgrowth in tomato (*SI Appendix*, Fig. S1). The *BIN2.2* loss-of-function mutant showed significant increases in total lateral bud length. Together with these bud outgrowth phenotypes, the levels of transcripts encoding *BRC1*, which is a central regulator suppressing shoot branching, were increased in the *dwf* and *bzr1* mutant buds and decreased in the buds of the *bin2.2* mutant as well as those of the *OE-DWF* and *OE-BZR1* plants (Fig. 1*C*). In agreement with these findings, histochemical analysis of β -glucuronidase (GUS) expression driven by *BRC1* promoter (P_{BRC1}) showed that the signal was greater in the *dwf* mutant than the WT (Fig. 1*D*). In situ hybridization studies showed that the levels of *BRC1* messenger RNA in the meristem and leaf primordia of the axillary buds were higher in the *dwf* mutant than the WT, whereas *BRC1* transcripts were barely detectable in the *OE-DWF* plants (Fig. 1*E*). Taken together, these results indicated that the growth of lateral buds is promoted by increasing the expression of BR biosynthesis and signaling genes in tomato.

BR-Induced Bud Outgrowth Is Not Attributable to Changes in the Levels of Auxin, SLs, and CKs. Given the roles of auxin, SLs, and CKs in bud growth, we next examined whether BR promotes bud

outgrowth by altering the levels of auxin, SLs, and CKs in tomato plants. The *dwf* mutant showed lower levels of indole-3-acetic acid (IAA) in nodal stems and roots than the WT, while *OE-DWF* plants showed increased IAA levels in roots without differences in the IAA levels in the stems (Fig. 1*F*). Consistent with the observations of root IAA levels, the expression of the auxin-responsive reporter gene *DR5::GUS* was decreased in the root tips of the *dwf* mutant and increased in the *OE-DWF* roots (*SI Appendix*, Fig. S2*A*). Compared to the WT, the expression of *CCD7*, *CCD8*, and *MAX1* was suppressed in the roots of the *dwf* mutant and increased in those of the *OE-DWF* plants (*SI Appendix*, Fig. S2*B*). In addition, the content of solanacol and dihydro-orabanchol was decreased in the *dwf* roots but increased in those of the *OE-DWF* plants (Fig. 1*G*). There were no significant differences in the orabanchol contents that accompanied the changes in the BR levels in different lines. In contrast to SLs, the levels of *Isopentenyltransferase2* (*IPT2*) transcripts in the nodal stems were inversely correlated with BR levels (*SI Appendix*, Fig. S2*B*). While *OE-DWF* plants did not show any changes in the CK content of the nodal stems, the accumulation of the bioactive CKs isopentenyladenosine (iP) and *trans*-zeatin (tZ) and of the ribosides isopentenyladenosine riboside (iPR), *trans*-zeatin riboside (tZR), and dihydro-zeatin riboside (DHZR) was significantly increased in the *dwf* mutant (Fig. 1*H*). As bud outgrowth is promoted by CKs and suppressed by auxin and SLs, it is unlikely that BR promotes bud outgrowth through impacts on IAA, SL, and CK homeostasis in tomato plants.

BR Signaling Directly Regulates the Expression of *BRC1*. Since the *dwf* and *bzr1* mutants showed increased *BRC1* expression in the lateral buds, we next determined whether BR signaling releases apical dominance by regulating the expression of *BRC1*. The *brc1* mutant generated by CRISPR/Cas9 showed a significantly increased total lateral bud length. However, knocking out *BRC1* in the *OE-DWF* plants did not further increase total lateral bud length (Fig. 2 *A* and *B*), suggesting that *BRC1* may be involved in BR-induced bud outgrowth. Silencing of *BRC1* released buds from dormancy in the *dwf* and *bzr1* mutants (Fig. 2 *C* and *D*) and resulted in a similar total lateral bud length in the *bzr1* mutant (but not the *dwf* mutant) to the WT. Furthermore, silencing of *DWF* or *BZR1* inhibited bud outgrowth in the WT but did not affect the total lateral bud length of the *brc1* mutant (*SI Appendix*, Fig. S3). These results indicate that *BRC1* acts downstream of BR signaling to regulate bud outgrowth.

Next, we examined whether BZR1 directly regulates the expression of *BRC1*. In the yeast one-hybrid (Y1H) assay (Fig. 2*E*), the yeast cells containing the P_{BRC1} -bait vector and the pGADT7-BZR1 vector grew on the SD/Leu media containing aureobasidin A (AbA). In contrast, transformants without BZR1 failed to grow on this media. There are five fragments (P1 to P5) containing E-box that are the potential binding sites for BZR1 in P_{BRC1} (Fig. 2*F*). Chromatin immunoprecipitation (ChIP)-qPCR analysis indicated that BZR1 bound to the P4 fragment of the P_{BRC1} . Dual-luciferase assay showed that the activity of P_{BRC1} was inhibited by 67% as a result of BZR1 binding (Fig. 2*G*), whereas a mutation of the E-box in the P4 fragment abolished the regulatory effects of BZR1 on *BRC1* without changing the basal promoter activity. Collectively, these findings demonstrated that BZR1 binds to the P_{BRC1} at the E-box motif and then suppresses *BRC1* expression. This down-regulation of *BRC1* ultimately promotes bud outgrowth.

BR Signaling Is Required for Release of Apical Dominance in Buds. To study the role of BR signaling in apical dominance, we analyzed the response of lateral buds to decapitation, a traditional means to release apical dominance. Decapitation led to a rapid increase in the levels of transcripts of *DET2* and *DWF* that encode BR

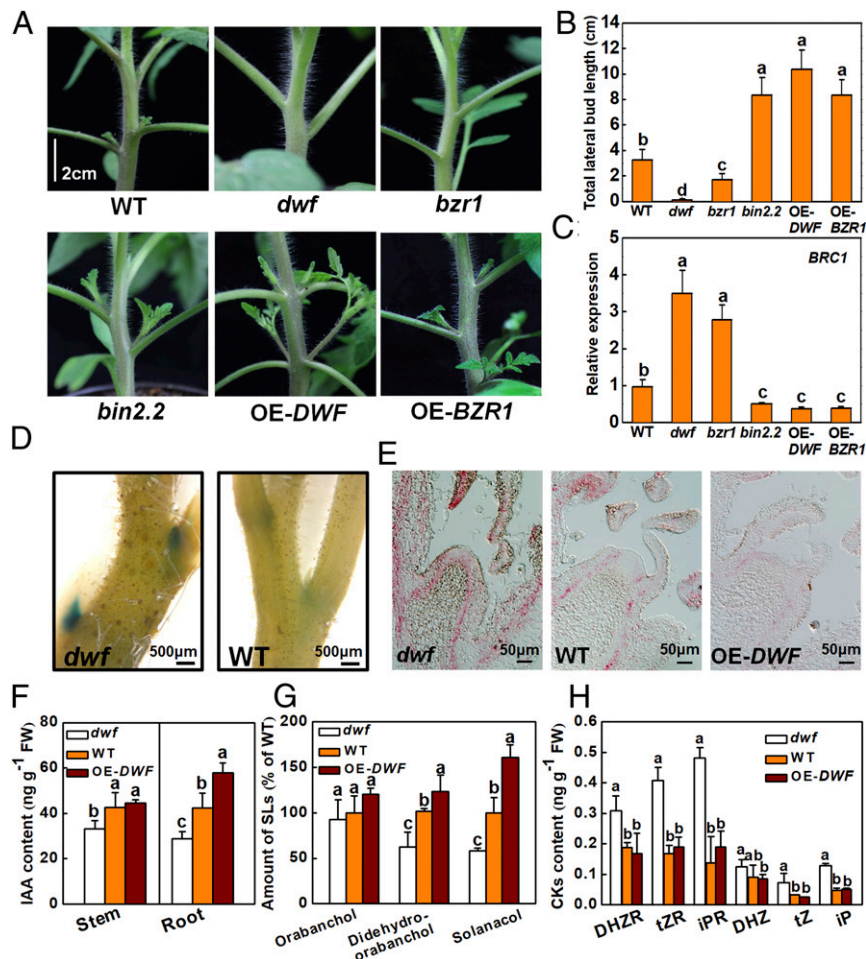


Fig. 1. BR signaling regulates bud outgrowth in tomato. (A and B) Bud outgrowth phenotypes of BR biosynthesis (*dwarf*) and signaling (*bsr1*, *bin2.2*) mutants and transgenic plants overexpressing BR biosynthesis gene *DWF* and signaling gene *BZR1*. (C) qPCR analysis of relative transcript of *BRC1* in axillary buds. (D) Histochemical analysis of GUS expression driven by P_{BRC1} . (E) In situ hybridization of messenger RNA of *BRC1* in axillary buds. (F) IAA content in nodal stems and roots. (G) Relative content of orobanchol, didehydro-orobanchol, and solanacol in roots. (H) CKs content in nodal stems of *dwarf* mutant, WT, and OE-*DWF* plants. Data are presented as the means of three replicates \pm SD. Different letters indicate significant differences ($P < 0.05$) according to Tukey's test.

synthesis enzymes. This increase was observed within 3 to 6 h of decapitation, while the levels of *CYP90B1* and *CPD* transcripts were either decreased or unaltered, respectively (Fig. 3A). Decapitation also resulted in the suppression of the expression of BR inactivation gene *CYP734A8* and the negative regulator signaling genes *BIN2.2* and *BIN2.3* in the buds. In addition, the levels of brassinolide (BL), the active end product of BR synthesis, were significantly increased in buds and nodes after decapitation (Fig. 3B). Moreover, an increase in the accumulation of the BZR1 protein, particularly the active form dBZR1, was observed in buds after decapitation (Fig. 3C). Treatment of buds with 24-epibrassinolide resulted in a similar increase in dBZR1 levels (*SI Appendix*, Fig. S4). Together, these findings suggest that the release from apical dominance is associated with enhanced BR signaling in buds.

After decapitation, the total length of lateral buds was increased in the WT and in the empty vector (EV) based on Tobacco Rattle Virus (TRV) plasmid (Fig. 3D and E and *SI Appendix*, Fig. S5). However, the suppression of lateral bud growth was not completely relieved by decapitation in the *dwarf* and *bsr1* mutants or the TRV-*BRI1* plants. The release from apical dominance in the WT and TRV plants was associated with the suppression of *BRC1* expression (Fig. 3F and G). However, the levels of *BRC1* transcripts remained higher in the buds of the

dwarf, *bsr1*, or TRV-*BRI1* plants than the WT or pTRV plants after decapitation. These results indicate that BR plays a crucial role in apical dominance.

BR Signaling Is Involved in Hormone- and Sucrose-Regulated Shoot Branching in Tomato.

Since auxin, SLs, CKs, and sugars are involved in apical dominance, we next studied whether BR mediates hormone and sugar signals for controlling the bud growth. Silencing of *FLOOZY* (*FZY*), which is an auxin synthesis gene, and cosilencing of *CCD7* and *CCD8* (*CCD7/8*) genes that are required for SL biosynthesis resulted in a significant increase in total length of lateral buds in the WT. Similarly, the application of 6-benzylaminopurine (6-BA, a synthetic CK) to buds at a concentration of 50 μ M or the application of sucrose to leaves at a concentration of 20 mM promoted lateral bud growth in the WT (Fig. 4A and B and *SI Appendix*, Figs. S6 and S7). In contrast to these observations, only minor to moderate increases in the total length of lateral buds were observed in the *dwarf* and *bsr1* mutants after silencing of *FZY* or *CCD7/8* or the application of 6-BA or sucrose. While the expression of *BRC1* was suppressed in the WT plants after silencing *FZY* or *CCD7/8*, or the application of 6-BA or sucrose, high levels of *BRC1* transcripts were observed in the *dwarf* and *bsr1* mutants, regardless of the loss of *FZY* and *CCD7/8* functions or the application of 6-BA and

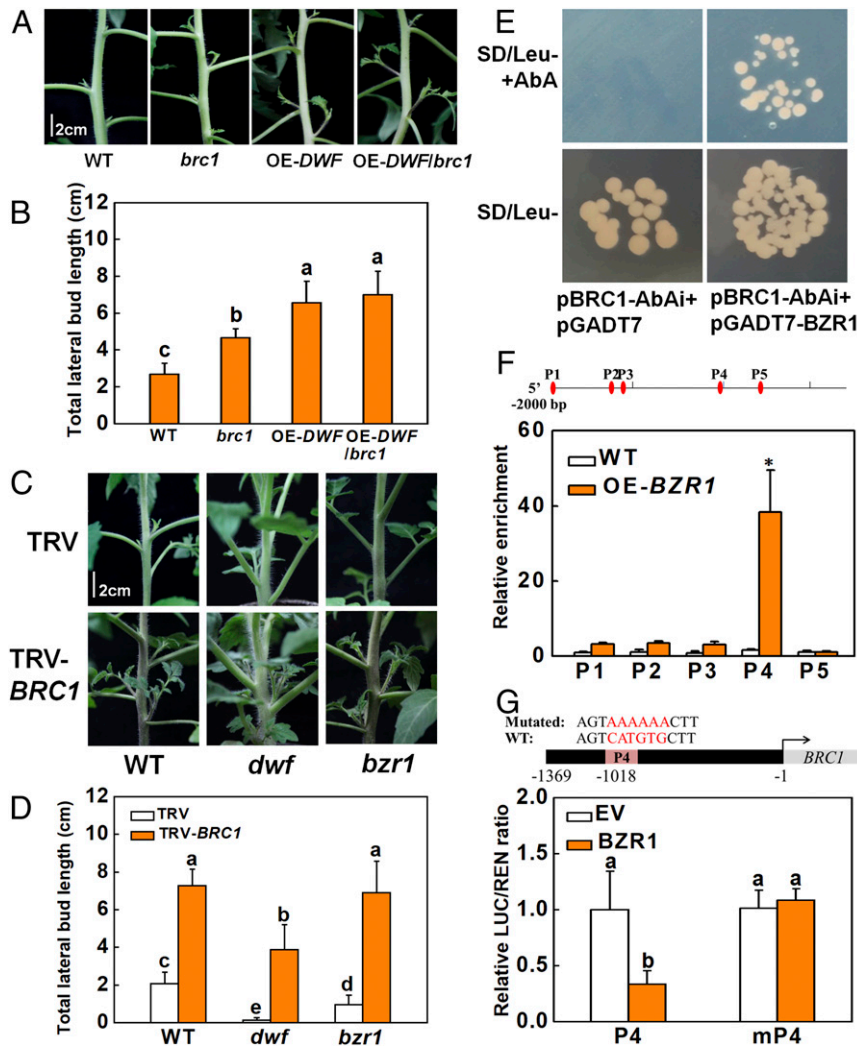


Fig. 2. BR signaling is involved in bud outgrowth through transcriptional regulation of *BRC1* by BZR1. (A and B) Bud outgrowth phenotypes of WT, *brc1* mutant, OE-DWF plants, and OE-DWF plants in the *brc1* background (OE-DWF/*brc1*). (C and D) Effects of silencing of *BRC1* on the bud outgrowth phenotypes of *dwf* and *bzc1* mutants. (E) Y1H analysis of BZR1 binding to the *P_{BRC1}*. (F) ChIP-qPCR analysis of BZR1 binding to the *P_{BRC1}*. P1 to P5 represented the DNA fragments containing the E-box in the *P_{BRC1}*. The asterisk indicated statistical difference between WT and OE-BZR1 plants (Student's *t* test, $P < 0.05$). (G) Dual-luciferase assay for the regulatory effect of BZR1 on the expression of *BRC1*. WT and mutated *P_{BRC1}* were used for the assay. The ratio of LUC/REN of the EV plus promoter was set as one. Data are presented as the means of three replicates \pm SD. Different letters indicate significant differences ($P < 0.05$) according to Tukey's test.

sucrose (Fig. 4 D and E). Decreasing auxin and SLs levels via VIGS or the application of 6-BA or sucrose resulted in enhanced accumulation of *DET2* and *DWF* transcripts (SI Appendix, Figs. S6 and S7), followed by increases in BL levels and the accumulation of the dBZR1 protein in the buds (Fig. 4 G, H, and J).

In contrast to the above observations, a significant decrease in total lateral bud length was observed in the *procera* (*pro*) mutant, which is defective in a DELLA protein, an inhibitor of GA signaling (Fig. 4C and SI Appendix, Fig. S8A). The levels of *BRC1* transcripts were increased, whereas the expression of BR biosynthesis genes (*DET2* and *DWF*) was decreased, together with a decrease in the BL contents in the buds of the *pro* mutant (Fig. 4 F and I and SI Appendix, Fig. S8B). In addition, silencing of *PRO* resulted in a decreased accumulation of dBZR1 (Fig. 4J). WT plants treated with the GA biosynthesis inhibitor (paclobutrazol [PAC]) showed an increase in total lateral bud length and decreased levels of *BRC1* transcripts. In contrast, PAC-induced bud growth was not observed in the *dwf* mutant (SI Appendix, Fig. S8 C–E). These data suggest that BR signaling is

involved in the hormone and sugar-regulated shoot branching in tomato.

CK Signaling Mediates Multiple Hormone and Sugar Signals to Promote BR Biosynthesis in Buds.

CKs have been extensively studied as promoters of shoot branching (11, 12). The decreases in the auxin and SLs levels of the *FZY*- and *CCD7/8*-silenced plants, as well as the sucrose treatment resulted in an increase in the levels of *IPT2* transcripts that encode the CK synthesis enzyme and in the total CK content in nodal stems (Fig. 5A and SI Appendix, Fig. S9A). The levels of CKs (iP, iPR, tZ, and tZR) were increased by cosilencing of *CCD7/8* or by sucrose treatment, while iP and tZR levels were increased by silencing *FZY*. In contrast, the levels of *IPT2* transcripts and the total CK contents were decreased in the *pro* mutant. Of the measured CKs, iP and tZR were decreased in the *pro* mutant (SI Appendix, Fig. S9 B–E).

Type-B RRs function as primary transcription factors in the regulation of gene expression in response to CKs (33). VIGS of *RR8*, *RR9*, *RR10*, *RR13*, and *RR21* revealed that only silencing of

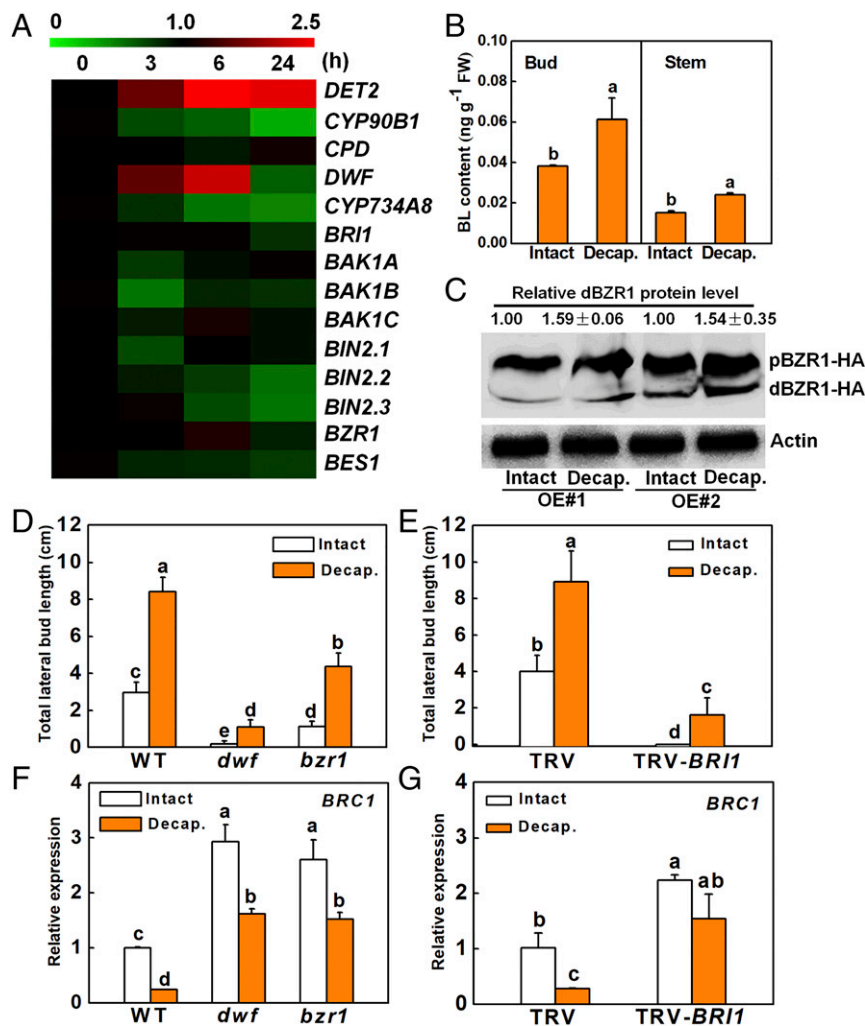


Fig. 3. BR signaling is required for the release from apical dominance. (A) Changes in transcript of BR biosynthesis and signaling genes in axillary buds in response to decapitation. (B) Changes in BL in axillary buds and nodal stems in response to decapitation. (C) Changes in relative accumulation of dBZR1, the active form involved in gene regulation, in axillary buds in response to decapitation. Signal intensity of dBZR1 protein was analyzed with ImageJ. The dBZR1 levels of control plants were set as one. (D and E) Effects of decapitation on the total lateral bud length of mutants in BR biosynthesis (*dwf*) and signaling (*bzt1*) or WT plants silenced for BR receptor gene *BRI1*. (F and G) qPCR analysis of the relative transcript of *BRC1* in axillary buds. Data are presented as the means of three replicates \pm SD. Different letters indicate significant differences ($P < 0.05$) according to Tukey's test.

RR10 significantly inhibited bud outgrowth (SI Appendix, Fig. S10). Based on these observations, *rr10* mutant was generated using CRISPR/Cas9. The *rr10* mutant showed a decrease in total lateral bud length, whereas overexpression of *RR10* (OE-*RR10*) significantly promoted bud outgrowth relative to the WT (Fig. 5 B and C). *BRC1* expression was increased in the *rr10* mutant but was suppressed in the OE-*RR10* plants (Fig. 5D). In addition, the *rr10* mutant was insensitive to 6-BA with regard to bud outgrowth. Moreover, the *RR10* protein levels were increased by 6-BA (SI Appendix, Fig. S11). Intriguingly, the expression of the key BR biosynthesis gene, *DWF*, was increased in the OE-*RR10* plants but suppressed in the *rr10* mutant. In agreement with these findings, OE-*RR10* resulted in an increase of BL contents in buds, whereas BL accumulation was decreased in the buds of *rr10* mutant (Fig. 5 E and F). However, no consistent changes in the levels of *DET2* transcripts were observed (SI Appendix, Fig. S12). Y1H assay and ChIP-qPCR analyses indicated that *RR10* directly bound to the promoter of *DWF* gene. Dual-luciferase assay confirmed the direct regulation of *DWF* expression by *RR10* (Fig. 5 G–I). Taken together, these results indicate that *RR10*-mediated CK response promotes BR

biosynthesis through transcriptional regulation of the *DWF* gene, leading to bud outgrowth in tomato.

Discussion

Shoot branching is generally considered to be controlled by the crosstalk between auxin, CKs, SLs, and sugars. Here, we provide evidence supporting that BR signaling is crucial to the control of shoot branching through the direct transcriptional suppression of *BRC1*. Auxin, CK, SL, and sugars impinge on a common BR–BZR1–*BRC1* cascade that regulates bud outgrowth. Furthermore, our results demonstrate that *RR10* mediates the CK response and regulates the expression of *DWF* to promote BR synthesis and bud outgrowth. Based on these findings, we propose a model in which BR signaling integrates hormonal and sugar signals to control shoot branching (Fig. 5J).

BR Signaling Is Essential for the Release of Apical Dominance by the Direct Suppression of *BRC1* Expression. The results presented in this study provide several lines of evidence showing that BR is directly involved in the regulation of bud outgrowth. Defects in BR synthesis (*DWF*) or in the positive regulator genes of BR

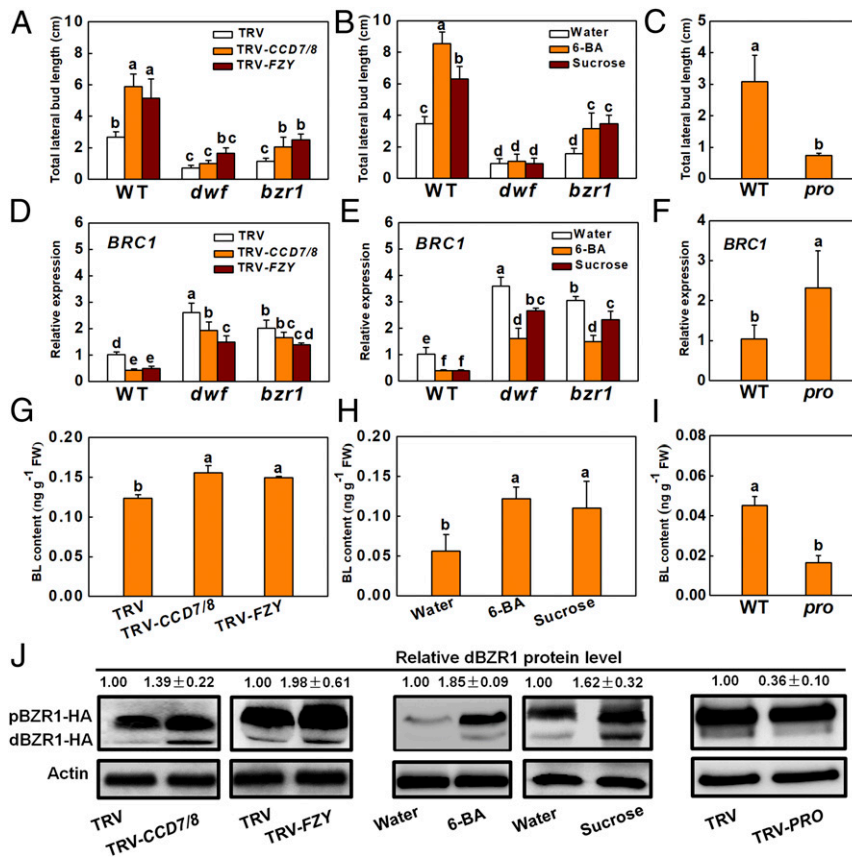


Fig. 4. BR signaling is involved in hormone and sugar-regulated bud outgrowth. (A) Effects of silencing of auxin biosynthesis gene *FZY* or cosilencing of SL biosynthesis genes *CCD7* and *CCD8* on the total lateral bud length of *dwf* and *bzr1* mutants. (B) Effects of application of 50 μ M 6-BA, a synthetic CK, to buds and foliar application of sucrose at 20 mM on the total lateral bud length of *dwf* and *bzr1* mutants. (C) Total lateral bud length of WT and DELLA-deficient *pro* mutant. (D–F) qPCR analysis of the relative transcript of *BRC1* in axillary buds. (G–I) Changes in BL in axillary buds. (J) Changes in relative accumulation of dBZR1 in axillary buds. The signal intensity of dBZR1 protein was analyzed with ImageJ. The dBZR1 levels of control or TRV plants were set as one. Data are presented as the means of three replicates \pm SD. Different letters indicate significant differences ($P < 0.05$) according to Tukey's test.

signaling (*BRI1* and *BZR1*) inhibited bud outgrowth. In contrast, OE-*DWF* or mutant in the negative regulator of BR signaling *BIN2.2* promoted lateral bud outgrowth (Figs. 1 and 3). Decapitation induced a rapid increase in the levels of transcripts encoding BR biosynthesis enzymes, together with decreases in transcripts involved in BR inactivation or negative regulation of BR signaling in the axillary buds. These changes were followed by increased levels of BL and dBZR1. However, decapitation was less effective in the suppression of *BRC1* expression and in the promotion of bud outgrowth in the *dwf* and *bzr1* mutants or when the BR receptor gene *BRI1* was silenced (Fig. 3). These findings suggest that BR signaling acts downstream of signals triggered by removal of shoot apex and that it is essential for the release of apical dominance.

Since no long-distance transport of BRs has been documented (34), BR signaling may act locally in buds to promote shoot branching. Indeed, *BRC1*, which is expressed in developing buds (8, 9), was found to be transcriptionally regulated by BR signaling. The results of a GUS reporter gene driven by the *BRC1* promoter (*P_{BRC1}::GUS*) expression, in situ hybridization, and qPCR analysis demonstrate that BR suppresses the expression of *BRC1* (Fig. 1). Molecular approaches provide further evidence that *BZR1* is the key component of BR signaling that mediates the transcriptional regulation of *BRC1* (Fig. 2). Importantly, we provide genetic evidence showing that *brc1* mutant does not show enhanced shoot branching in the OE-*DWF* background, whereas silencing of *BRC1* rescued the bud growth phenotypes in

the *dwf* and *bzr1* mutants, suggesting that *BRC1* acts downstream of BR in the regulation of shoot branching. These results indicate that BR regulates shoot branching at least in part through *BZR1*-dependent regulation of *BRC1* expression in lateral buds. Since the presence of *BRC1* alone is not sufficient to prevent bud outgrowth in some cases (35), the incomplete recovery of bud growth achieved by the silencing of *BRC1* in the *dwf* mutant suggests that BR may regulate bud growth through both *BRC1*-dependent and -independent routes. Since BR is a well-known regulator of cell division and elongation (36), these processes may be involved in BR-induced bud outgrowth.

BR Signaling Is Regulated by Hormone and Sugar Signals Involved in Apical Dominance. Accumulating evidence has demonstrated the intensive crosstalk between auxin, SL, CK, and sugars in the control of apical dominance. In this regulatory network, auxin and SL act as repressors, while CK and sugars act as inducers of shoot branching (7, 11). In the present study, we found that the *dwf* mutant showed a decreased accumulation of IAA in the nodal stem, together with lower SL levels in the roots and an increased accumulation of CKs in the nodal stem (Fig. 1). These findings suggest that BR-dependent regulation of bud growth is not attributable to changes in auxin, SL, or CK levels. However, these hormones may regulate BR synthesis and signaling, which promote bud outgrowth.

The results presented here show that silencing of *FZY* or *CCD7* and *CCD8*, which are involved in auxin and SL synthesis,

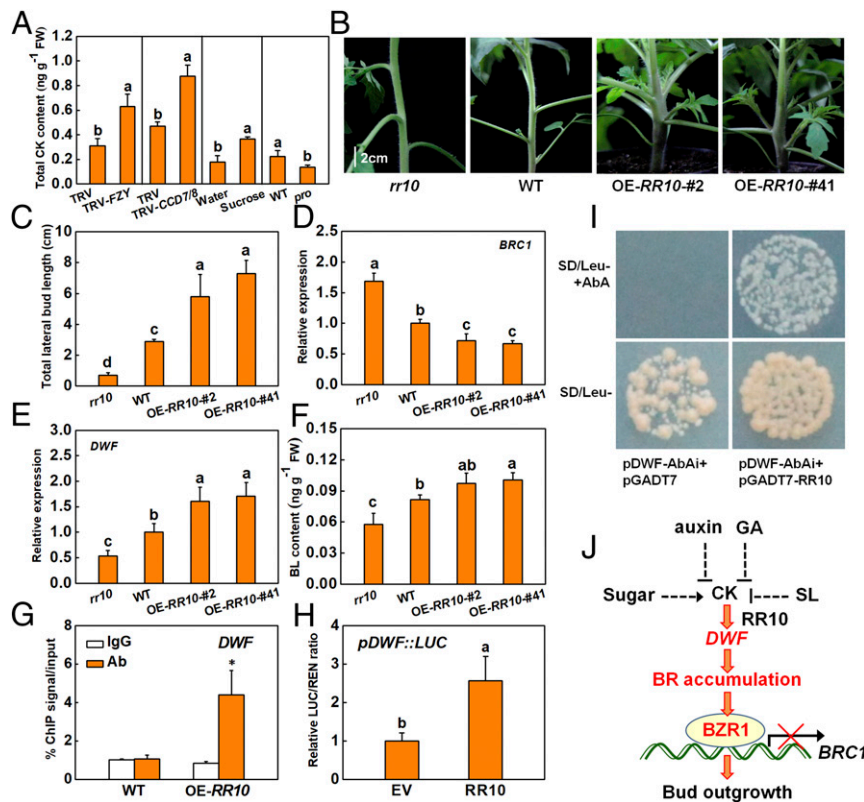


Fig. 5. CK signaling regulates BR biosynthesis in axillary buds. (A) Effects of silencing of *FZY* or cosilencing of *CCD7/8*, treatment of 6-BA (50 μ M) or foliar application of sucrose at 20 mM, and enhanced GA signaling in *pro* mutant on total CK content in nodal stems. (B and C) Bud outgrowth phenotypes of *rr10* mutant and plants OE-*RR10*, which encodes a type-B RR in CK signaling. (D) qPCR analysis of the relative transcript of *BRC1* in axillary buds. (E) qPCR analysis of the relative transcript of BR biosynthesis gene *DWF* in axillary buds. (F) Changes in BL in axillary buds. (G) ChIP-qPCR analysis of RR10 binding to the *DWF* promoter. The asterisk indicated statistical difference between WT and OE-*BZR1* plants (Student's *t* test, $P < 0.05$). (H) Dual-luciferase assay for the regulatory effect of RR10 on the expression of *DWF*. The ratio of LUC/REN of the EV plus promoter was set as one. Data are presented as the means of three replicates \pm SD. Different letters indicate significant differences ($P < 0.05$) according to Tukey's test. (I) Y1H analysis of RR10 binding to the *DWF* promoter. (J) The model in which BR signaling integrates multiple hormone and sugar signals to promote bud outgrowth. Auxin, SL, and GA reduce, while CK increases BR accumulation in axillary buds. BR activates *BZR1*, which transcriptionally suppresses *BRC1*, resulting in bud outgrowth. CK promotes BR biosynthesis through transcriptional activation of *DWF* with the action of RR10. Arrows indicate activation, and blunt-ended lines indicate inhibition.

stimulated bud growth, together with an increased abundance of *DET2* and *DWF* transcripts and an increase in BL levels and *BZR1* accumulation in the axillary buds. The observed increases in bud outgrowth were compromised in mutants that are defective in BR synthesis (*dwf*) or signaling (*bzr1*) (Fig. 4). These results indicate that BR signaling is essential for the auxin- and SL-dependent regulation of bud growth. The synthesis and/or signaling of BR and auxin show reciprocal regulation (37). Decreases in auxin resulting from decapitation resulted in a down regulation of the BR biosynthesis gene *CYP90B1* and the catabolism gene *CYP734A8* (Fig. 3). These findings are consistent with earlier findings that auxin increases the expression of *CYP90B1* and *CYP734A1* in *Arabidopsis* roots (38, 39). However, further studies are required to fully understand the mechanisms by which auxin signaling regulates BR accumulation in buds. We found that SLs negatively regulate the expression of BR biosynthesis genes as well as the accumulation of BL and *BZR1* (Fig. 4). These findings are consistent with an earlier observation that SLs activated MAX2, a subunit of an SCF E3 ligase, promotes the degradation of *BZR1* protein in *Arabidopsis* (40). We conclude that BR mediates SL signaling in the regulation of shoot branching. Suppression of SL synthesis genes in the *dwf* mutant (Fig. 1) may be due to feedback regulation. Like auxin, GA has also been shown to be involved in the control of apical dominance (21, 41). The DELLA-deficient *pro* mutant showed reduced shoot branching with lower BR signaling in buds.

Moreover, bud growth arising from the inhibition of GA synthesis by PAC was abolished in the *dwf* mutant (Fig. 4 and *SI Appendix*, Fig. S8). These results confirm the role of BR in apical dominance and indicate that GA inhibits BR signaling in axillary buds, possibly through increased auxin sensitivity (42).

Earlier studies have demonstrated that sugar availability is critical for regulating apical dominance (19, 43). We found that the application of sucrose to leaves promotes bud outgrowth, together with increased expression of BR synthesis genes and accumulation of BL and *BZR1* (Fig. 4 and *SI Appendix*, Fig. S7). However, sucrose-driven bud growth was largely compromised in the *dwf* and *bzr1* mutants, indicating that BR synthesis and signaling are required for sugar-induced shoot branching in tomato. Recently, mutations in the BR synthesis gene *DET2* were found to compromise hypocotyl elongation in response to sugars (44). Moreover, the stability of *BZR1* was shown to be regulated by the sugar-activated target of rapamycin protein kinase in *Arabidopsis* (45). Taken together, these results suggest that sugar acts as a signal in the regulation of BR biosynthesis and signaling in diverse developmental processes, including shoot branching.

CK Signaling Directly Regulates BR Biosynthesis. Auxin in the nodal stem inhibits CKs synthesis (12), while D53, a central regulator of SL signaling, was recently shown to regulate CK degradation (46). In addition, increased sugar availability positively regulates CK synthesis (43). Consistent with previous studies, the results

presented here show that CKs are regulated by auxin, SLs, GA signaling, and sucrose in tomato (Fig. 5). Based on these results, it will be interesting to study the mechanism whereby CK mediates auxin, SL, and sugar signals to regulate BR synthesis. CKs regulate hormone crosstalk through the action of type-B RRs (47, 48). Loss of *RR10* functions suppressed bud outgrowth in tomato, whereas OE-*RR10* promoted bud outgrowth (Fig. 5). In addition, we present evidence showing that *RR10* is essential for CK-induced bud growth (SI Appendix, Fig. S11). The results of a series of physiological and molecular studies demonstrate that *RR10* directly promotes BR synthesis by the transcriptional activation of *DWF* gene in tomato (Fig. 5). In this way, *RR10*-mediated BR synthesis integrates hormone and sugar signals to regulate shoot branching. CKs are known to suppress the expression of *BRC1*, while the mechanisms involved in the transcriptional regulation of *BRC1* by CK signaling remain unclear (49). Our results indicate that CK signaling may regulate the expression of *BRC1* through BR synthesis. Notably, CKs play an important role in shoot branching, but they are not absolutely required for bud growth in response to decapitation (50). BR functions locally in buds and may be more closely coupled with the release of apical dominance. Other signals such as SLs and sugars may also regulate BR synthesis and signaling through CK-dependent and CK-independent pathways to control shoot branching.

In conclusion, the data presented here show that BR is required for the release of apical dominance. BR does not promote bud growth through decreasing apical dominance, but rather it acts locally in buds to suppress the expression of *BRC1* through the action of *BZR1*. Traditional signals involved in apical dominance such as auxin, SLs, CKs, and sugars, together with GA regulate BR biosynthesis in buds. In addition, auxin, SL, sugar, and GA may regulate BR via CK, which regulates BR synthesis through *RR10*-mediated transcriptional activation of *DWF* gene (Fig. 5). Based on these findings, together with the results of previous studies, we propose that BR signaling integrates multiple pathways in the regulation of shoot branching.

Materials and Methods

Plant Materials and Growth Conditions. The *dwf* and *pro* mutants, together with the corresponding WT, *Solanum lycopersicum* cv. (cultivar) Condine Red and cv. Ailsa Craig were obtained from Tomato Genetics Resource Center (<https://tgrc.ucdavis.edu>). Condine Red was used as the WT for CRISPR/Cas9 mutants and transgenic plants. Transgenic plants overexpressing *DWF* and OE-*BZR1*, and CRISPR/Cas9 mutant of *bzr1* were generated during previous studies (51, 52). Seeds were germinated in Petri dishes at 28 °C and the germinated seeds were sown in a mixture of peat and vermiculite (2:1, volume/volume [vol/vol]). When the plants had grown to the two-leaf stage, they were transferred to pots (height × diameter, 15 cm × 10 cm) containing the same substrate. The plants were grown in a controlled growth chamber with 12 h light (200 μmol m⁻² · s⁻¹) at 23 °C and 12 h dark at 20 °C. The relative humidity was kept at 70%. Plants were watered with Hoagland nutrient solution every 2 d.

IGS. For gene silencing, complementary DNA (cDNA) fragments of target genes were amplified using primers listed in SI Appendix, Table S1. Purified PCR products were cloned into TRV2 vector. After confirmation by sequencing, the plasmids were transformed into *Agrobacterium tumefaciens* strain GV3101. When the cotyledons fully expanded, the seedlings were infiltrated with a mixture of *A. tumefaciens* strain carrying a TRV2 derivative and the strain carrying the helper vector TRV1 as previously described (53). The infiltrated plants were kept in the aforementioned growth chamber. qPCR was performed to ensure silencing efficiency before experiments.

Cloning Procedures and Plant Transformation. CRISPR/Cas9 system was used to generate *bin2.2*, *brc1*, and *rr10* mutants as previously described (54). The single guide RNA (sgRNA) sequences were designed by the CRISPR-P program (crispr.hzau.edu.cn/CRISPR2/) as follows: *BIN2.2*: ACCTCAGCACCATAA-TCCGC; *BRC1*: TCTTCTCTGTATGCAATA; *RR10*: GGGTCTGTTCTCAGTTCGAC.

The synthesized sgRNA sequence was annealed and introduced into BbsI site of an AtU6-sgRNA-AtUBQ-Cas9 vector. The resulting plasmid was

digested by HindIII and KpnI and then inserted into pCAMBIA1301 binary vector digested by the same restriction enzymes. After confirmation by sequencing, the vector containing sgRNA and Cas9 was transformed into *A. tumefaciens* strain GV3101. Plant transformation was performed as described previously (51). Primers used for genotyping were as follows: *BIN2.2*: TGAGAACACGAGAAAAATAT and ACTACCTTTTCGGATTCCATT; *BRC1*: ATCACCTTTGGTCAATCCA and TCATCTCTTTCTTTTCG; *RR10*: GTAAGATAA-ACCCCAAAAAAG and CTCATAGTGACAGTCTTGAGC.

An insertion of one base pair (bp) was found in the +38, +70, and +33 position in the coding sequence of *BIN2.2*, *BRC1*, and *RR10*, respectively. The homozygous lines were used in this study.

To generate plants expressing *P_{BRC1}::GUS*, a 1,369 bp *P_{BRC1}* sequence was amplified by PCR using specific primers (SI Appendix, Table S2). The PCR product was ligated into the pBI121 vector, which harbors the GUS reporter gene. After confirmation by sequencing, the vector was transformed into *A. tumefaciens* strain GV3101, which was used for plant transformation. The *RR10*-OE plants were generated as described previously (51). The full-length coding sequence of *RR10* was amplified with the primers as shown in SI Appendix, Table S2. T3 homozygous lines generated from T1 individuals carrying a single insertion of the transgene were used in this study. The *P_{BRC1}::GUS* transgene was introduced into the *dwf* mutant and the *35S::DWF* transgene was introduced into the *brc1* mutant by crossing.

Treatments and Measurement of Lateral Bud Length. Treatments of plants were performed when plants have five fully expanded leaves. For decapitation, young leaves and shoot apex above the fifth node were removed by a sterilized scalpel. Nodes were numbered acropetally from the first true leaf. For 6-BA treatment, 22.5 mg 6-BA (Sigma-Aldrich, Merck Life Science Co.) was dissolved in 10 mL NaOH solution (0.1 M) and diluted with 40 mL distilled water to make a 2 mM 6-BA stock solution, then the stock solution was diluted 40 folds to make a 50 μM working solution. The 6-BA solution was applied in a volume of 10 μL directly to the axillary buds every two days. For sugar feeding, 20 mM sucrose solution was sprayed to fully expanded leaves of the whole plant. Each plant was treated with 15 mL sucrose solution twice a day until the end of the experiment. For the treatment of GA synthesis inhibitor PAC, PAC (Supelco, Merck Life Science Co.) was firstly dissolved in a minimum volume of ethanol to make a stock solution and then diluted with distilled water to make a 20 μM PAC working solution. The PAC solution was sprayed to fully expanded leaves of the whole plant in a volume of 15 mL. The treatment was applied twice a day until the end of the experiment. The length of lateral buds was measured 7 d after different treatments using a numeric caliper, perpendicular to the stem.

Histochemical GUS Analysis. For GUS staining, transgenic plants bearing the *P_{BRC1}::GUS* were fixed in 50 mM phosphate buffer (pH 7.0) containing 1% (vol/vol) formaldehyde and 0.04% Triton-X 100 for 30 min. After washing twice with phosphate buffer, samples were incubated at 37 °C overnight with GUS staining solution (50 mM phosphate buffer, pH 7.0, 0.4 mg · mL⁻¹ 5-bromo-4-chloro-3-indolyl-β-D-glucuronic acid, 1 mM potassium ferricyanide, and 1 mM potassium ferrocyanide). Following staining, samples were washed with a graded ethanol series to extract chlorophyll. Expression of *P_{BRC1}::GUS* was observed using a Zeiss STEMI305 stereo microscope.

In Situ Hybridization. Tomato axillary buds (about 2 mm) were fixed with 4% paraformaldehyde at 4 °C overnight, washed with phosphate buffer three times (5 min each), dehydrated through an ethanol series (30%, 50%, 70%, 80%, 90%, 95%, and 100%) for 30 min in each solution, and then treated with 100% ethanol for 1 h. After that, samples were treated through a graded series of xylene in ethanol (25%, 50%, 75%, and 100%), washed with 50% paraffin in xylene at 65 °C for 1 h, incubated at 65 °C with 100% paraffin overnight, embedded in paraffin in molds (MEIKO EC 360), and allowed to solidify at room temperature. Paraffin blocks were cut into 8 μm sections using a Manual Rotary Microtome (Thermo Scientific HM 325) and collected on adhesion microscope slides (MeVid). After dewaxing, in situ hybridization was performed using the RNAScope 2.5 HD Detection Kit (Advanced Cell Diagnostics [ACD]) following the manufacturer's protocol. *BRC1* probe and a negative control probe for an irrelevant bacterial gene *dapB* were provided by ACD. Slides were imaged on a Zeiss Axio Scope A1 microscope (Zeiss) with a Zeiss Axiocam 503 color camera and Zeiss ZEN imaging software.

Y1H Assay. Y1H assay was performed using Matchmatch Gold Yeast One-Hybrid System (Clontech) according to the manufacturer's instructions. *BRC1* or *DWF* promoter was ligated into the pAbAi vector and the full-length coding region of *BZR1* or *RR10* was also amplified using specific

primers (*SI Appendix, Table S2*) and fused to the pGADT7 vector. The linearized pAbAi constructs containing *BRC1* or *DWF* promoter were transformed into Y1HGold yeast strain. pGADT7-BZR1, pGADT7-RR10, or an empty AD vector was transformed into the modified Y1HGold yeast strain. The transformed yeast cells were selected on SD/Leu– media supplemented with 50 ng · mL⁻¹ AbA.

ChIP-qPCR. ChIP assay was performed using the EpiQuik Plant ChIP Kit (Epigentek). One gram of buds was fixed in 1% formaldehyde for 10 min under a vacuum and neutralized with glycine. After washing three times with cold sterilized water, the tissues were homogenized. Following isolation and sonication of chromatin, BZR1-HA (hemagglutinin) or RR10-HA protein was immunoprecipitated using anti-HA antibody. The enriched DNA was amplified by qPCR using specific primers (*SI Appendix, Table S3*). Enrichment was calculated by percentage of the immunoprecipitated DNA relative to the input. The goat anti-mouse immunoglobulin G (IgG) was used as the negative control. Relative enrichment was calculated by the ratio of the percentage of anti-HA–immunoprecipitated DNA to the percentage of IgG–immunoprecipitated DNA.

Dual-Luciferase Assay. Dual-luciferase assay was used to confirm BZR1 binding to the *P_{BRC1}* and RR10 binding to the *DWF* promoter according to a previous study (55). *BRC1* and *DWF* promoters were amplified and ligated into the pGreen II 0800-LUC vector (*SI Appendix, Table S2*). A variant of *P_{BRC1}*, which contains a mutation in the BZR1-binding site, was generated using overlapping PCR, in which two amplified fragments with an intended mutation in the overlapping region are joined together by PCR (56). The primer pairs used to create mutations are as follows (substituted nucleotides are underlined): reverse: 5'-CGTGAAGTAAATAAAGTTTTTACTTTGTCCATCC-TGAGCCG-3'; forward: 5'-CGGCTCAGGATGACAAAGTAAAAAATTTTATTTA-CCTCACG-3'.

The full-length coding region of *BZR1* or *RR10* was amplified and fused to the pGreen II 0029 62-SK vector (*SI Appendix, Table S2*). The above constructs were transformed into *A. tumefaciens* strain GV3101. To determine the activity of promoter as influenced by transcription factor, a mixture of *A. tumefaciens* strain carrying the pGreen II 0800-LUC vector or pGreen II 0029 62-SK vector in a 1:1 ratio was infiltrated into *Nicotiana benthamiana* leaves. Three days later, the activity of promoter was measured by the ratio of enzyme activity of firefly luciferase (LUC) and renilla luciferase (REN), which acted as an internal reference. The LUC/REN value in the absence of BZR1 or RR10 protein was set as one. Measurements were carried out using a Modulus Luminometer (Promega).

Measurement of Phytohormones. For measurement of IAA, 0.1 g samples were collected and homogenized in 1 mL ethyl acetate, which was spiked with D₆-IAA (C/D/N Isotopes Inc.) as internal standards. The homogenates were shaken overnight at 4 °C and centrifuged at 13,000 rpm for 10 min. The supernatants were transferred to new tubes and the pellets were resuspended in 1 mL ethyl acetate. The suspensions were shaken for 1 h and then centrifuged at 13,000 rpm for 10 min. The supernatants were combined and dried under gaseous N₂ flush. Samples were dissolved in 0.5 mL 70% methanol (vol/vol) for analysis.

SLs measurement was performed according to the method of Ruiz-Lozano et al. (57) with modifications. Root samples (0.5 g) were ground in a mortar filled with liquid nitrogen and then extracted with 0.5 mL 40% acetone (vol/vol). The homogenates were vortexed for 2 min and centrifuged at 8,000 g for 5 min. The supernatants were discarded, and the pellets were extracted twice with 0.5 mL 50% acetone (vol/vol). The supernatants were filtered through membrane filters (0.22 μm) and then analyzed.

For analysis of CKs, samples (0.2 g) frozen in liquid N₂ were ground to fine powders and then ground in 1 mL ice-cold extraction solution (15:1:4 [vol/vol/vol] methanol: formic acid: water), which was spiked with [²H₆]N⁶-iP, [²H₆]N⁶-iPR, [²H₃]-dihydrozeatin, [²H₃]-DHZR, [²H₅]-tZ, and [²H₅]-tZR. The extracts were kept at -30 °C overnight and centrifuged at 10,000 g for

15 min. The supernatants were collected and flowed through a hydrophilic lipophilic balance column (Oasis) which was pretreated with formic acid (1 M). An aliquot of 0.3 mL extraction solution was flowed through the column. The liquid was collected and dried under gaseous N₂ flush. Samples were dissolved in 1 mL formic acid (1 M) and flowed through a mixed-mode cation (MCX) column (Oasis) which was pretreated with formic acid (1 M). The column was washed sequentially with 1 mL formic acid (1 M), 1 mL methanol, 1 mL ammonia solution (0.35 M), and 1 mL 60% methanol containing 0.35 M ammonia. The final liquid was dried under gaseous N₂ flush and dissolved in 200 μL 1% acetic acid. The mixture was vortexed and then analyzed.

For measurement of BL, 0.1g bud or stem samples were ground into powder with liquid N₂ and then ground in 1 mL ice-cold acetonitrile, which was spiked with [26-²H₃]BL (Olchemim) as internal standard. After being extracted overnight at 4 °C, the homogenate was centrifuged at 10,000 g for 10 min at 4 °C. The supernatant was transferred into a new tube which contained 0.3g MCX@BBII and 3 mL ddH₂O and was vortexed for 5 min. MCX@BBII was prepared according to Luo et al. (58). After centrifugation at 10,000 g for 1 min at 4 °C, the pellet was resuspended with 5 mL 90% acetone which contained 0.5% formic acid and vortexed for 1 min. The mixture was centrifuged at 10,000 g for 1 min at 4 °C. The supernatant was discarded, and 1.2 mL 90% acetone followed by 20 to 50 mg ammonium acetate was added to the tube. The mixture was vortexed for 1 min and centrifuged at 10,000 g for 3 min. The upper phase was dried under mild N₂ flow and was dissolved in 100 μL 45% acetonitrile for analysis.

Phytohormones except BL were analyzed by Agilent 1290 ultra-high performance liquid chromatography coupled to 6460 triple quadrupole mass spectrometer. BL was analyzed by using ACQUITY ultra performance liquid chromatography I-Class coupled to Waters Xevo TQ-XS triple quadrupole mass spectrometer.

Western Blot. Protein extraction from bud samples and Western blot were performed as described previously (52). For Western blot, proteins were separated by SDS-PAGE using 10% (wt/vol) acrylamide gels and electrophoretically transferred to nitrocellulose membranes (Millipore). The BZR1-HA and RR10-HA proteins were detected with commercial antibodies raised against anti-HA monoclonal antibody (Thermo Fisher Scientific).

Gene Expression Analysis. Total RNA extraction was performed using an RNAPrep pure Plant Kit (TIANGEN) according to the operation manual. The first-strand cDNA was synthesized using ReverTraAce qPCR Reverse Transcription Kit with genome-DNA-removing enzyme (Toyobo). qPCR was performed on LightCycler480 detection system (Roche) using SYBR Super Mix (Takara, RR420A). Primers for target genes were shown in *SI Appendix, Table S4*. Tomato housekeeping gene *Actin* was used as internal reference. Relative expression of target genes was calculated according to Livak and Schmittgen (59).

Statistical Analysis. The experimental design was a completely randomized design. Data were subjected to statistical analysis of variance using the SPSS package (SPSS 19.0). The differences between the means were separated by Tukey's test at a level of *P* < 0.05.

Data Availability. All study data are included in the article and/or *SI Appendix*.

ACKNOWLEDGMENTS. This work was supported by the National Key Research and Development Program (2019YFD1001900), the National Natural Science Foundation of China (31672139), and the China Earmarked Fund for Modern Agro-industry Technology Research System (CARS-25). We thank Ms. Q. Sun for generating the *rr10* mutant and OE-*RR10* plants. We are also thankful to Dr. X. D. Wu for the help in phytohormone analysis and Dr. Z. Y. Qi for the maintenance of the growth chambers. WT tomato expressing *DR5::GUS* were kindly provided by M. G. Ivanchenko of Oregon University.

1. T. Sakamoto et al., Erect leaves caused by brassinosteroid deficiency increase biomass production and grain yield in rice. *Nat. Biotechnol.* **24**, 105–109 (2006).
2. Y. Q. Jiao et al., Regulation of *OssPL14* by *OsmiR156* defines ideal plant architecture in rice. *Nat. Genet.* **42**, 541–544 (2010).
3. B. Wang, S. M. Smith, J. Y. Li, Genetic regulation of shoot architecture. *Annu. Rev. Plant Biol.* **69**, 437–468 (2018).
4. B. Janssen, R. S. M. Drummond, K. C. Snowden, Regulation of axillary shoot development. *Curr. Opin. Plant Biol.* **17**, 28–35 (2014).
5. E. S. Martin-Fontecha, C. Tarancon, P. Cubas, To grow or not to grow, a power-saving program induced in dormant buds. *Curr. Opin. Plant Biol.* **41**, 102–109 (2018).

6. F. F. Barbier, E. A. Dun, S. C. Kerr, T. G. Chabikwa, C. A. Beveridge, An update on the signals controlling shoot branching. *Trends Plant Sci.* **24**, 220–236 (2019).
7. C. Rameau et al., Multiple pathways regulate shoot branching. *Front. Plant Sci.* **5**, 741 (2015).
8. J. A. Aguilar-Martinez, C. Poza-Carrión, P. Cubas, *Arabidopsis BRANCHED1* acts as an integrator of branching signals within axillary buds. *Plant Cell* **19**, 458–472 (2007).
9. M. Martin-Trillo et al., Role of tomato *BRANCHED1*-like genes in the control of shoot branching. *Plant J.* **67**, 701–714 (2011).
10. P. Prusinkiewicz et al., Control of bud activation by an auxin transport switch. *Proc. Natl. Acad. Sci. U.S.A.* **106**, 17431–17436 (2009).

11. D. Müller, O. Leyser, Auxin, cytokinin and the control of shoot branching. *Ann. Bot.* **107**, 1203–1212 (2011).
12. M. Tanaka, K. Takei, M. Kojima, H. Sakakibara, H. Mori, Auxin controls local cytokinin biosynthesis in the nodal stem in apical dominance. *Plant J.* **45**, 1028–1036 (2006).
13. V. Gomez-Roldan *et al.*, Strigolactone inhibition of shoot branching. *Nature* **455**, 189–194 (2008).
14. M. Umehara *et al.*, Inhibition of shoot branching by new terpenoid plant hormones. *Nature* **455**, 195–200 (2008).
15. T. Waldie, H. McCulloch, O. Leyser, Strigolactones and the control of plant development: Lessons from shoot branching. *Plant J.* **79**, 607–622 (2014).
16. S. Al-Babili, H. J. Bouwmeester, Strigolactones, a novel carotenoid-derived plant hormone. *Annu. Rev. Plant Biol.* **66**, 161–186 (2015).
17. P. B. Brewer, E. A. Dun, B. J. Ferguson, C. Rameau, C. A. Beveridge, Strigolactone acts downstream of auxin to regulate bud outgrowth in pea and *Arabidopsis*. *Plant Physiol.* **150**, 482–493 (2009).
18. A. Hayward, P. Stirnberg, C. Beveridge, O. Leyser, Interactions between auxin and strigolactone in shoot branching control. *Plant Physiol.* **151**, 400–412 (2009).
19. M. G. Mason, J. J. Ross, B. A. Babst, B. N. Wienclaw, C. A. Beveridge, Sugar demand, not auxin, is the initial regulator of apical dominance. *Proc. Natl. Acad. Sci. U.S.A.* **111**, 6092–6097 (2014).
20. T. H. Kebrom *et al.*, Inhibition of tiller bud outgrowth in the *tin* mutant of wheat is associated with precocious internode development. *Plant Physiol.* **160**, 308–318 (2012).
21. S. F. Lo *et al.*, A novel class of gibberellin 2-oxidases control semidwarfism, tillering, and root development in rice. *Plant Cell* **20**, 2603–2618 (2008).
22. W. Huang *et al.*, Overexpression of a tomato miR171 target gene *SIGRAS24* impacts multiple agronomical traits via regulating gibberellin and auxin homeostasis. *Plant Biotechnol. J.* **15**, 472–488 (2017).
23. A. P. Singh, S. Savaldi-Goldstein, Growth control: Brassinosteroid activity gets context. *J. Exp. Bot.* **66**, 1123–1132 (2015).
24. Y. Belkhadir, Y. Jaillais, The molecular circuitry of brassinosteroid signaling. *New Phytol.* **206**, 522–540 (2015).
25. Y. Sun *et al.*, Integration of brassinosteroid signal transduction with the transcription network for plant growth regulation in *Arabidopsis*. *Dev. Cell* **19**, 765–777 (2010).
26. U. K. Divi, T. Rahman, P. Krishna, Gene expression and functional analyses in brassinosteroid-mediated stress tolerance. *Plant Biotechnol. J.* **14**, 419–432 (2016).
27. Q. F. Li *et al.*, The brassinosteroid-regulated transcription factors BZR1/BES1 function as a coordinator in multisignal-regulated plant growth. *Biochim. Biophys. Acta. Gene Regul. Mech.* **1861**, 561–571 (2018).
28. C. Y. Wu *et al.*, Brassinosteroids regulate grain filling in rice. *Plant Cell* **20**, 2130–2145 (2008).
29. M. Mori *et al.*, Isolation and characterization of a rice dwarf mutant with a defect in brassinosteroid biosynthesis. *Plant Physiol.* **130**, 1152–1161 (2002).
30. H. N. Tong *et al.*, DWARF AND LOW-TILLERING, a new member of the GRAS family, plays positive roles in brassinosteroid signaling in rice. *Plant J.* **58**, 803–816 (2009).
31. Z. Fang *et al.*, Strigolactones and brassinosteroids antagonistically regulate the stability of the D53-OsBZR1 complex to determine *FC1* expression in rice tillering. *Mol. Plant* **13**, 586–597 (2020).
32. J. Hu, Y. Ji, X. Hu, S. Sun, X. Wang, BES1 Functions as the co-regulator of D53-like SMXLs to inhibit *BRC1* expression in strigolactone-regulated shoot branching in *Arabidopsis*. *Plant Commun.* **1**, 100014 (2019).
33. R. D. Argyros *et al.*, Type B response regulators of *Arabidopsis* play key roles in cytokinin signaling and plant development. *Plant Cell* **20**, 2102–2116 (2008).
34. G. M. Symons, J. B. Reid, Brassinosteroids do not undergo long-distance transport in pea. Implications for the regulation of endogenous brassinosteroid levels. *Plant Physiol.* **135**, 2196–2206 (2004).
35. M. Seale, T. Bennett, O. Leyser, *BRC1* expression regulates bud activation potential but is not necessary or sufficient for bud growth inhibition in *Arabidopsis*. *Development* **144**, 1661–1673 (2017).
36. M. P. González-García *et al.*, Brassinosteroids control meristem size by promoting cell cycle progression in *Arabidopsis* roots. *Development* **138**, 849–859 (2011).
37. H. Tian, B. Lv, T. Ding, M. Bai, Z. Ding, Auxin-BR interaction regulates plant growth and development. *Front. Plant Sci.* **8**, 2256 (2018).
38. Y. Chung *et al.*, Auxin stimulates *DWARF4* expression and brassinosteroid biosynthesis in *Arabidopsis*. *Plant J.* **66**, 564–578 (2011).
39. J. Chaiwanon, Z. Y. Wang, Spatiotemporal brassinosteroid signaling and antagonism with auxin pattern stem cell dynamics in *Arabidopsis* roots. *Curr. Biol.* **25**, 1031–1042 (2015).
40. Y. Wang *et al.*, Strigolactone/MAX2-induced degradation of brassinosteroid transcriptional effector BES1 regulates shoot branching. *Dev. Cell* **27**, 681–688 (2013).
41. G. W. Bassel, R. T. Mullen, J. D. Bewley, *Procera* is a putative DELLA mutant in tomato (*Solanum lycopersicum*): Effects on the seed and vegetative plant. *J. Exp. Bot.* **59**, 585–593 (2008).
42. E. Oh *et al.*, Cell elongation is regulated through a central circuit of interacting transcription factors in the *Arabidopsis hypocotyl*. *eLife* **3**, e03031 (2014).
43. F. Barbier *et al.*, Sucrose is an early modulator of the key hormonal mechanisms controlling bud outgrowth in *Rosa hybrida*. *J. Exp. Bot.* **66**, 2569–2582 (2015).
44. Y. Zhang *et al.*, Brassinosteroid is required for sugar promotion of hypocotyl elongation in *Arabidopsis* in darkness. *Planta* **242**, 881–893 (2015).
45. Z. Zhang *et al.*, TOR signaling promotes accumulation of BZR1 to balance growth with carbon availability in *Arabidopsis*. *Curr. Biol.* **26**, 1854–1860 (2016).
46. J. Duan *et al.*, Strigolactone promotes cytokinin degradation through transcriptional activation of *CYTOKININ OXIDASE/DEHYDROGENASE 9* in rice. *Proc. Natl. Acad. Sci. U.S.A.* **116**, 14319–14324 (2019).
47. I. Hwang, J. Sheen, B. Müller, Cytokinin signaling networks. *Annu. Rev. Plant Biol.* **63**, 353–380 (2012).
48. Y. O. Zubo *et al.*, Cytokinin induces genome-wide binding of the type-B response regulator ARR10 to regulate growth and development in *Arabidopsis*. *Proc. Natl. Acad. Sci. U.S.A.* **114**, E5995–E6004 (2017).
49. E. A. Dun, A. de Saint Germain, C. Rameau, C. A. Beveridge, Antagonistic action of strigolactone and cytokinin in bud outgrowth control. *Plant Physiol.* **158**, 487–498 (2012).
50. D. Müller *et al.*, Cytokinin is required for escape but not release from auxin mediated apical dominance. *Plant J.* **82**, 874–886 (2015).
51. X. J. Li *et al.*, *DWARF* overexpression induces alteration in phytohormone homeostasis, development, architecture and carotenoid accumulation in tomato. *Plant Biotechnol. J.* **14**, 1021–1033 (2016).
52. Y. L. Yin *et al.*, BZR1 transcription factor regulates heat stress tolerance through FERONIA receptor-like kinase-mediated reactive oxygen species signaling in tomato. *Plant Cell Physiol.* **59**, 2239–2254 (2018).
53. F. Wang *et al.*, Phytochrome A and B function antagonistically to regulate cold tolerance via abscisic acid-dependent jasmonate signaling. *Plant Physiol.* **170**, 459–471 (2016).
54. C. Pan *et al.*, CRISPR/Cas9-mediated efficient and heritable targeted mutagenesis in tomato plants in the first and later generations. *Sci. Rep.* **6**, 24765 (2016).
55. X. R. Yin *et al.*, Involvement of an ethylene response factor in chlorophyll degradation during citrus fruit degreening. *Plant J.* **86**, 403–412 (2016).
56. Y. Zhang, S. Dorey, M. Swiderski, J. D. G. Jones, Expression of *RPS4* in tobacco induces an AvrRps4-independent HR that requires EDS1, SGT1 and HSP90. *Plant J.* **40**, 213–224 (2004).
57. J. M. Ruiz-Lozano *et al.*, Arbuscular mycorrhizal symbiosis induces strigolactone biosynthesis under drought and improves drought tolerance in lettuce and tomato. *Plant Cell Environ.* **39**, 441–452 (2016).
58. X. T. Luo, B.-D. Cai, L. Yu, J. Ding, Y.-Q. Feng, Sensitive determination of brassinosteroids by solid phase boronate affinity labeling coupled with liquid chromatography-tandem mass spectrometry. *J. Chromatogr. A* **1546**, 10–17 (2018).
59. K. J. Livak, T. D. Schmittgen, Analysis of relative gene expression data using real-time quantitative PCR and the 2(-Δ Δ C(T)) Method. *Methods* **25**, 402–408 (2001).